Dnm1 forms spirals that are structurally tailored to fit mitochondria

Elena Ingerman,[1] Edward M. Perkins,[2] Michael Marino,[3] Jason A. Mears,[3] J. Michael McCaffery,[2] Jenny E. Hinshaw,[3] and Jodi Nunnari[1]

[1]Department of Molecular and Cellular Biology, Center for Genetics and Development, University of California, Davis, Davis, CA 95616
[2]Department of Biology and Integrated Imaging Center, Johns Hopkins University, Baltimore, MD 21218
[3]Laboratory of Cell Biochemistry and Biology, National Institute of Arthritis, Diabetes, and Digestive and Kidney Diseases, National Institutes of Health (NIH), Bethesda, MD 20892

Dynamin-related proteins (DRPs) are large self-assembling GTPases whose common function is to regulate membrane dynamics in a variety of cellular processes. Dnm1, which is a yeast DRP (Drp1/Dlp1 in humans), is required for mitochondrial division, but its mechanism is unknown. We provide evidence that Dnm1 likely functions through self-assembly to drive the membrane constriction event that is associated with mitochondrial division. Two regulatory features of Dnm1 self-assembly were also identified. Dnm1 self-assembly proceeded through a rate-limiting nucleation step, and nucleotide hydrolysis by assembled Dnm1 structures was highly cooperative with respect to GTP. Dnm1 formed extended spirals, which possessed diameters greater than those of dynamin-1 spirals but whose sizes, remarkably, were equal to those of mitochondrial constriction sites in vivo. These data suggest that Dnm1 has evolved to form structures that fit the dimensions of mitochondria.

Introduction

The mechanism underlying dynamin-related protein (DRP)–dependent membrane remodeling events is still largely unknown. Experimental work on dynamin, which functions during endocytosis in the scission of clathrin-coated pits from the plasma membrane (Hinshaw, 2000; Song and Schmid, 2003; Praefcke and McMahon, 2004), has revealed that all DRPs contain three functionally important and distinct domains: a GTPase domain, a smaller middle domain, and a COOH-terminal assembly or GTPase effector domain (GED; Muhlberg et al., 1997; van der Bliek, 1999). The association of these domains via intra- and inter-molecular interactions promotes the self-assembly of dynamin into higher order filamentous and spiral-like structures and stimulates GTP hydrolysis to a relatively high rate (Warnock et al., 1996; Muhlberg et al., 1997; Sever et al., 1999; Smirnova et al., 1999; Marks et al., 2001; Zhu et al., 2004). In vivo, self-assembly is required for dynamin's ability to remodel membranes during endocytosis (Song et al., 2004). In vitro, the assembly of dynamin on spherical lipid vesicles causes them to constrict and deform into dynamin–lipid tubes (Hinshaw and Schmid, 1995; Takei et al., 1998; Kim et al., 2001; Zhang and Hinshaw, 2001; Kochs et al., 2002; Chen et al., 2004). Studies of other DRPs have shown that they also can self-assemble, suggesting that this feature is characteristic and functionally important (Zhang et al., 2000; Yoon et al., 2001; Zhu et al., 2004). Based on the ability of dynamin to self-assemble and on its kinetic properties, it has been postulated to play a mechanochemical role in severing endocytic vesicles from the plasma membrane (Hinshaw and Schmid, 1995; Marks et al., 2001; Song and Schmid, 2003). However, other findings suggest that dynamin functions as a classic signaling GTPase, which, in its GTP-bound form, recruits downstream effectors that are responsible for membrane division (Sever et al., 1999, 2000; Newmyer et al., 2003). Thus, although the mechanism of clathrin vesicle scission is still unclear, it is likely that dynamin plays two roles during endocytosis: that of a regulatory GTPase during rate-limiting early events of coated pit formation and maturation and that of a transducer of mechanochemical work during membrane fission and vesicle formation (Narayanan et al., 2005).

Like dynamin, the yeast DRP Dnm1 is also required for a membrane scission event—mitochondrial division. Dnm1 is found in punctate structures, which are targeted to the outer mitochondrial membrane and are localized at sites of mitochondrial division (Shaw and Nunnari, 2002; Osteryoung and Nunnari, 2003). It has been postulated that Dnm1-containing structures, which are products of self-assembly, function to drive the membrane constriction and fission events that are

Correspondence to Jodi Nunnari: jmnunnari@ucdavis.edu; or Jenny E. Hinshaw: jennyh@helix.nih.gov

Abbreviations used in this paper: DRP, dynamin-related protein; GDP, guanosine 5′-diphosphate; GED, GTPase effector domain; GMP-PCP, β,γ-methyleneguanosine 5′-triphosphate; PEP, phosphoenolpyruvate.

The online version of this article contains supplemental material.

The Journal of Cell Biology, Vol. 170, No. 7, September 26, 2005 1021–1027
http://www.jcb.org/cgi/doi/10.1083/jcb.200506078

associated with mitochondrial division (Tieu and Nunnari, 2000). Dnm1-dependent mitochondrial division, however, is also regulated by and requires the actions of the outer membrane protein Fis1 and the WD repeat adaptor proteins Mdv1 and Caf4 (Fekkes et al., 2000; Mozdy et al., 2000; Tieu and Nunnari, 2000; Cerveny et al., 2001; Tieu et al., 2002; Suzuki et al., 2005). At least one essential function of Fis1 in mitochondrial fission is to target and sequester Mdv1 and Caf4 on the mitochondrial outer membrane (Tieu and Nunnari, 2000; Tieu et al., 2002; Cerveny and Jensen, 2003; Griffin et al., 2005). After targeting, the Fis1–Mdv1 complex interacts with assembled Dnm1 to trigger mitochondrial division (Tieu and Nunnari, 2000; Tieu et al., 2002). The Fis1–Caf4 complex also functions to facilitate fission, but with significantly less efficacy (Griffin et al., 2005). Thus, the role of the Fis1–Caf4 complex in mitochondrial division is most likely regulatory. To begin to unravel the mechanism of mitochondrial division, we have characterized the kinetic and structural properties of Dnm1. Our observations suggest that Dnm1 self-assembly drives the constriction of mitochondria during division and reveal novel characteristics of DRPs that likely allow for their regulation in vivo.

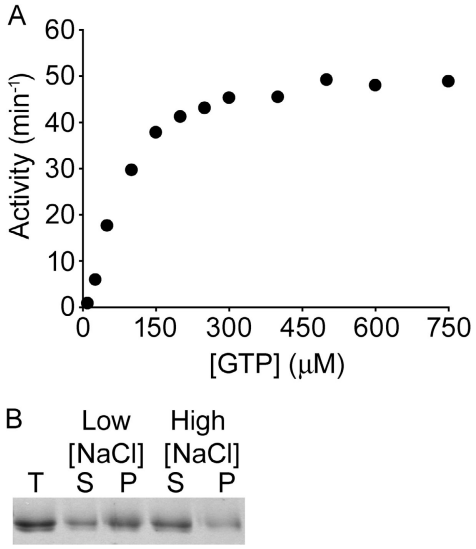

Figure 1. **Kinetics and velocity sedimentation of Dnm1.** (A) Steady-state kinetics of Dnm1 GTPase activity under assembly conditions. 0.06 mg/ml Dnm1 was assayed for GTPase activity at 150 mM NaCl. (B) Velocity sedimentation of Dnm1 at low and high ionic strength. T, total; S, supernatant; P, pellet.

Results and discussion

Dnm1 exhibits a lag in reaching steady-state assembly-dependent GTPase activity

Previous studies using recombinant Dnm1 and Drp1/Dlp1 from *Escherichia coli* demonstrated that they hydrolyze GTP and self-interact (Fukushima et al., 2001; Yoon et al., 2001). For more detailed kinetic and structural characterization, we purified a greater yield of active protein recombinant Dnm1 from baculovirus-infected insect cells. We examined the ability of Dnm1 to hydrolyze GTP, initially using a fixed time point assay with α-[^{32}P]GTP followed by the TLC-based separation of products (Fukushima et al., 2001). However, observing that the rate of GTP hydrolysis, especially at low GTP concentrations, is limited by substrate depletion, we used a coupled assay in which GTP was continuously regenerated from guanosine 5′-diphosphate (GDP; Renosto et al., 1984) to obtain more accurate GTP hydrolysis rate measurements.

Using this assay, we determined the steady-state kinetics of Dnm1 GTPase activity at relatively low ionic strength conditions, which are predicted to favor self-assembly (Fig. 1 A and Table I). Under these conditions, Dnm1 demonstrated a relatively high rate of GTP hydrolysis and a relatively low affinity for GTP, which is consistent with kinetic parameters that were previously observed for assembled dynamin (Sever et al., 1999; Song and Schmid, 2003). Indeed, an examination of Dnm1 assembly by velocity sedimentation analysis revealed that at low ionic strength and in contrast to its behavior at high ionic strength, Dnm1 quantitatively assembled into large particles, which were recovered in the pellet fraction (Fig. 1 B). Consistent with Dnm1 self-assembly, GTP hydrolysis was also cooperative with respect to Dnm1 concentration (Fig. S1 A, available at http://www.jcb.org/cgi/content/full/jcb.200506078/DC1).

Significantly, we also observed that GTP hydrolysis is cooperative with respect to GTP concentration, suggesting that GTP-dependent conformational and regulatory changes occur within assembled Dnm1 structures under steady-state conditions (Table I). This cooperation has not been observed previously for other DRPs possibly because of substrate-limiting

Table I. **Kinetic and hydrodynamic[a] parameters of Dnm1 and Dnm1 mutants**

Parameters	Wild-type Dnm1 (high ionic strength)[b]	Wild-type Dnm1 (low ionic strength)[b]	Dnm1 1–388 (GTPase domain)	Dnm1G385D
k_{cat} (min^{-1})[c]	11.6	50.7	0.84	3.11
$K_{0.5}/K_m$ (μM)[c]	214	79.1	19.2	109.9
Hill coefficient	3.3	1.6	1	1
Kinetic lag	+	+	–	–
Ve (mL)[d]	9.54	ND	16.9	13.1
Stokes' radius (A)[e]	130	ND	33.0	73.2
Sedimentation coefficient (S)[f]	18.6	ND	2.7	5.7
Molecular mass (kD)[g]	995	ND	36.6	174
Estimated number of subunits[h,i]	10	ND	1	2

[a]Dnm1G385D and GTPase domain at 500 mM NaCl. Wild-type Dnm1 at 750 mM NaCl.
[b]High ionic strength, 500 mM NaCl; low ionic strength, 150 mM NaCl.
[c]Calculated by nonlinear least squares method using the GenFit function of Mathcad.
[d]Superose 6 column.
[e]Calculated based on Porath correlation of gel filtration standards.
[f]Calculated based on native high molecular mass markers.
[g]Estimated by using the method developed by Siegel and Monty (1966).
[h]Subunit estimation based on the unmodified molecular mass of the protein, which was determined by mass spectrometry (87 kD).
[i]Rounded to nearest subunit. Actual values are as follows: Dnm1G385D, 2.0; Dnm1 GTPase domain, 0.92; and wild-type Dnm1, 10.4.

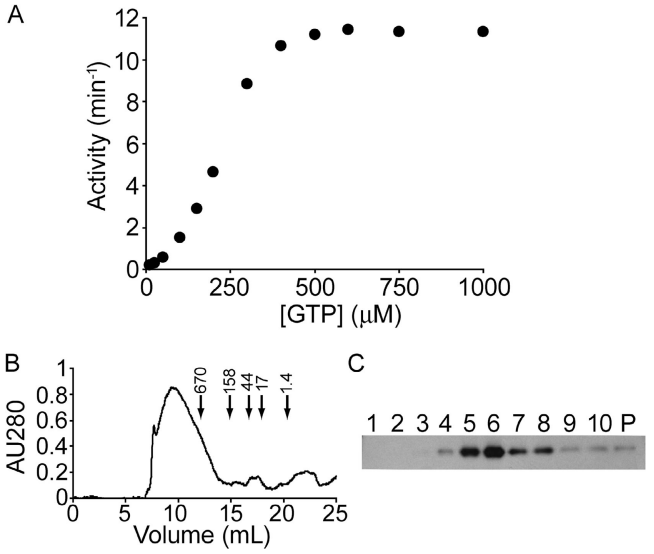

Figure 2. **High ionic strength antagonizes Dnm1 self-assembly and reveals GTP-dependent cooperation.** (A) Steady-state kinetics of Dnm1 at high ionic strength. 0.06 mg/ml Dnm1 was assayed for GTPase activity at 500 mM NaCl. (B) Gel filtration analysis of Dnm1 using a Superose 6 column at 750 mM NaCl. (C) Sucrose gradient sedimentation of Dnm1 (from which the blot was created). Fractions collected from a 5–20% sucrose gradient were analyzed by Western blot analysis using anti-Dnm1 antibodies. Native high molecular mass markers were used to create a standard curve. Sedimentation coefficients of the protein standards were plotted versus the mean sucrose gradient fraction number in which the protein standard appeared. Molecular mass standards with sedimentation coefficients in parentheses that were distributed in sucrose gradient fractions are listed as follows (top, fraction 1; bottom, fraction 10): BSA (4.3 S), fraction 2.3; lactate dehydrogenase (7.4 S), fraction 3.3; catalase (11.3 S), fraction 4.6; and thyroglobulin (19.4 S), fraction 6.9. P, pellet.

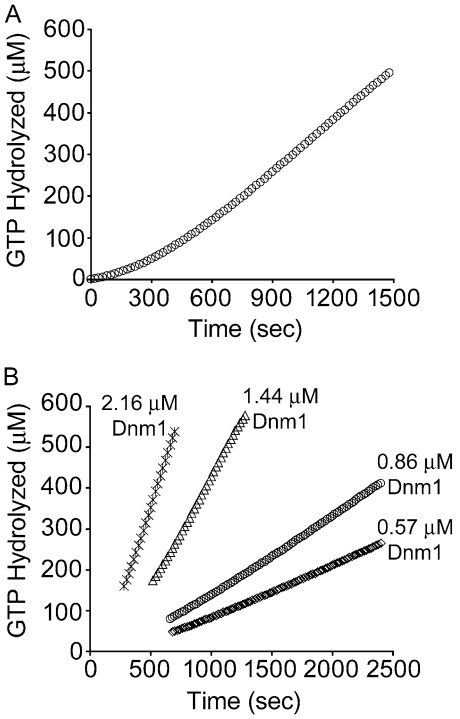

Figure 3. **Nucleation-dependent assembly of Dnm1.** (A) Time dependence of Dnm1 GTPase activity at low ionic strength. GTPase assay was initiated by the dilution of Dnm1at high ionic strength into low ionic strength GTPase assay buffer. (B) Dnm1 concentration dependence of lag time. Indicated concentrations of Dnm1 were assayed at low ionic strength. Only steady-state regions of plots of GTPase activity versus time are shown to demonstrate a decrease in lag time with increasing Dnm1 concentration.

conditions of the assays that were used for their characterization. Interestingly, at high ionic strength, during which Dnm1 self-assembly was antagonized and the rate of GTP hydrolysis was lower than that found at low ionic strength, GTP-dependent cooperation of Dnm1 was greatly increased (Fig. 2 A and Table I). This observation raises the possibility that GTP-dependent cooperation is harnessed to drive early events in Dnm1 self-assembly. To test this, we examined the hydrodynamic properties of Dnm1 at high ionic strength (Fig. 2, B and C; and Table I). We observed that under these conditions, Dnm1 is present quantitatively at a steady state in structures that range in size from 8 to 12 mer. Thus, at high ionic strength, Dnm1 is present in an assembled, albeit smaller, structure. These observations, coupled with the observed GTP-dependent cooperation of Dnm1, imply that GTP-dependent cooperation in GTPase activity is a characteristic of assembled Dnm1.

Monitoring GTP hydrolysis continuously as permitted by our coupled assay after the addition of Dnm1 from high to low ionic strength conditions allowed us to observe a significant and reproducible lag of 300–600 s in reaching steady-state GTP hydrolysis velocity (Fig. 3 A). In self-assembling systems, such a kinetic lag is a hallmark of a rate-limiting nucleation event and also has not been previously observed for DRPs. Consistent with this interpretation, we found that kinetic lag is dependent on Dnm1 concentration, decreasing with increasing Dnm1 concentration (Fig. 3 B). This observation suggests that, initially, and in a rate-limiting manner, Dnm1 nucleates its own self-assembly into a higher order structure. The structure of the proposed nucleator is currently unknown, but our hydrodynamic analysis of Dnm1 at high ionic strength indicates that it contains >8–12 Dnm1 subunits.

The assembly-defective mutant Dnm1G385D exists as a stable dimer that exhibits no kinetic lag and no cooperation with respect to protein or substrate concentration

To test whether kinetic lag reflects a Dnm1 nucleation-dependent self-assembly event and to gain further insight into the pathway for Dnm1 assembly, we characterized Dnm1G385D, which contains a point mutation in a conserved residue in the middle domain of Dnm1 (for review see Jensen et al., 2000). In contrast to Dnm1, which is present in punctate structures in yeast cells, Dnm1G385 possesses a diffuse cytosolic distribution and does not support mitochondrial fission, suggesting that it fails to self-assemble in vivo and that self-assembly is essential for mitochondrial division (for review see Jensen et al., 2000).

Characterization of the GTPase activity of Dnm1G385D at low ionic strength revealed that the turnover of GTP was significantly reduced relative to Dnm1 at either low or high ionic strength and was also not dependent on Dnm1G385D concen-

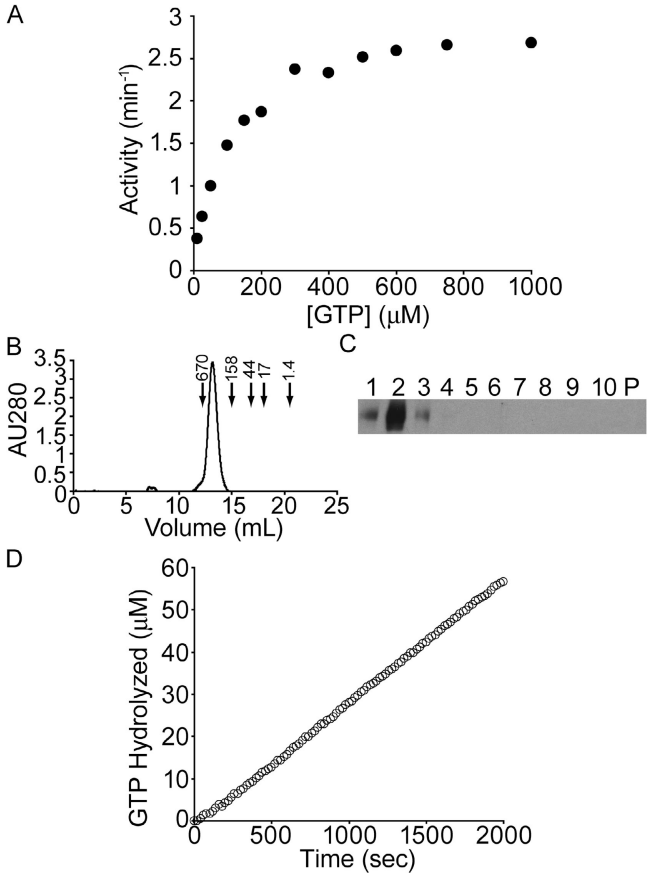

Figure 4. **Dnm1G385D is an assembly-deficient dimer.** (A) Steady-state kinetics of 0.08 mg/ml Dnm1G385D at 150 mM NaCl. (B) Gel filtration analysis of Dnm1G385D using a Superose 6 column at 500 mM NaCl. (C) Sucrose gradient sedimentation of Dnm1G385D (from which the blot was created). Fractions collected from a 10–30% sucrose gradient were analyzed as described in Fig. 2. Molecular mass standards with sedimentation coefficients stated in parentheses that were distributed in sucrose gradient fractions are listed as follows (top, fraction 1; bottom, fraction 10): BSA (4.3 S), fraction 1.6; lactate dehydrogenase (7.4 S), fraction 2.5; catalase (11.3 S), fraction 3.5; and thyroglobulin (19.4 S), fraction 5.1. (D) Time dependence of Dnm1G385D GTPase activity under experimental conditions that were similar to those of wild-type Dnm1.

tration, suggesting that self-assembly of Dnm1G385D is deficient in vitro (Fig. 4 A, Fig. S1 B, and Table I). Consistent with its relatively low GTPase activity, an examination of the subunit composition of Dnm1G385D by hydrodynamic analysis indicated that higher order assembled structures were not formed and, instead, that Dnm1G385D existed as a stable and discrete dimer (Fig. 4, B and C; and Table I). Significantly, continuous monitoring of Dnm1G385D GTPase activity revealed no lag in reaching steady-state GTPase velocity (Fig. 4 D and Table I) over a broad Dnm1G385D concentration range (not depicted). These observations support our interpretation that the lag observed for Dnm1 GTPase activity indeed reflects the self-assembly of a nucleation structure. Interestingly, we also observed a lag phase for dynamin-1 (Fig. S2, available at http://www.jcb.org/cgi/content/full/jcb.200506078/DC1). Our findings raise the intriguing possibility that the regulation of Dnm1 nucleation may be a key event in mitochondrial division and may be a general mechanism for the regulation of DRP function as it is for the function of other filaments such as F-actin and microtubules.

In contrast to Dnm1, kinetic characterization indicated that Dnm1G385D possessed a Hill coefficient of 1, indicating an absence of cooperation with respect to GTP (Fig. 4 A and Table I). Thus, it is possible that positive cooperation is a feature that is unique to higher order Dnm1 assembled structures. Alternatively, Dnm1G385D may be defective for GTP-dependent cooperation and, as a consequence, may fail to undergo a conformational change that orients it for assembly. In either case, GTP-dependent positive cooperation is likely to be important in vivo, where it might function as a switch that drives Dnm1 self-assembly to facilitate mitochondrial constriction and division. This switch may be regulated by intracellular concentrations of GTP or, alternatively, may be used by other mitochondrial-localized division proteins such as Mdv1 that interact with Dnm1 and target it to mitochondria to drive Dnm1 self-assembly in a spatially regulated manner.

We examined the structural requirements for Dnm1 dimer formation by characterizing the Dnm1 GTPase domain. Hydrodynamic characterization of the Dnm1 GTPase domain (Dnm1 1–338), which lacks the middle and GED domains, indicates that Dnm1 1–338 exists as a stable monomer (Table I). Kinetic analysis of Dnm1 1–338 indicated that like Dnm1G385D, Dnm1 1–338 possesses no kinetic lag and is less active than Dnm1G385D (Table I). Thus, although Dnm1G385D fails to assemble into higher order Dnm1 structures, intermolecular interactions between GED and/or middle and GTPase domains are still required for the formation of a stable dimer and for an intermediate level of activation of GTP hydrolysis. Our kinetic analyses of Dnm1, Dnm1G385D, and the Dnm1 GTPase domain also indicate that fully activated GTP hydrolysis in higher order Dnm1 structures results from more complex intermolecular interactions between more than two adjacent Dnm1 subunits.

Altogether, our observations suggest that dimeric Dnm1 functions as the building block for Dnm1 higher order structures and that Dnm1G385D forms a terminal dimer that is unable to support assembly, pointing to the critical function of the middle domain in the assembly of Dnm1 into higher order structures. Consistent with this interpretation is the observation that Dnm1G385D is a dominant-negative inhibitor of mitochondrial fission in vivo and of Dnm1 GTPase activity in vitro (Fig. S3, available at http://www.jcb.org/cgi/content/full/jcb.200506078/DC1). A dimeric building block for Dnm1 higher order structures may be different from dynamin, whereas hydrodynamic analyses suggest that the building block is a tetramer. However, a cryo-EM structure of assembled dynamin suggests that although dynamin tetramers exist, dynamin dimers are the fundamental units in higher order spiral structures (Zhang and Hinshaw, 2001; Chen et al., 2004).

Dnm1 forms rings and spirals possessing diameters that match in vivo mitochondrial constrictions

One feature of the model that has been postulated for DRP-mediated mitochondrial division is that the assembly of a spiral-

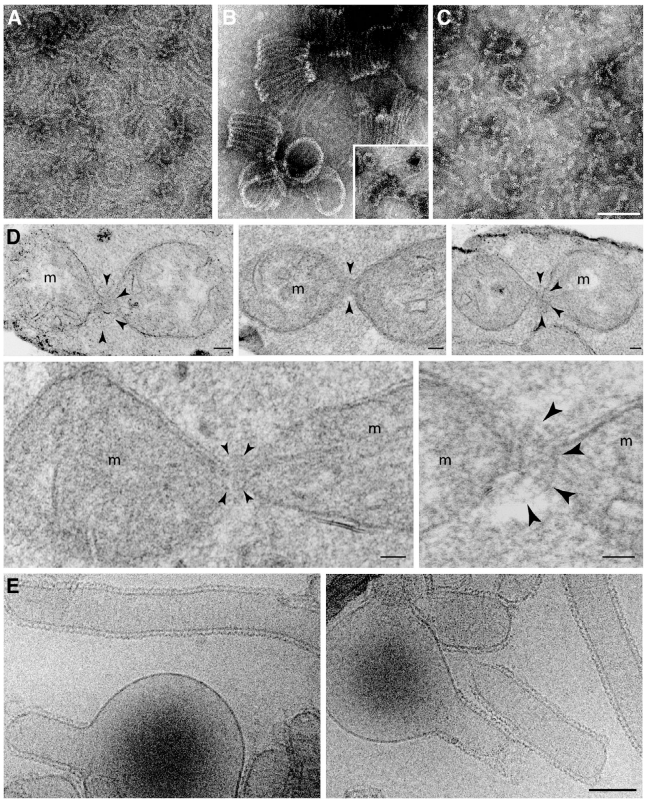

Figure 5. **Dnm1 self-assembles into spirals that are structurally tailored to fit mitochondria.** (A–C) Electron micrographs of negatively stained Dnm1 structures. (A) Dnm1 forms curved filaments in the absence of nucleotides. (B) Dnm1 self-assembles into large spirals in the presence of GMP-PCP. (Inset) Dynamin-1 spirals formed in the presence of GDP/BeF_x. (C) Dnm1/GMP-PCP spirals undergo a conformational change upon the addition of GTP. (D) Conventional EM analysis of mitochondrial constriction sites in thin sections of yeast cells. Arrowheads indicate electron-dense structures that are found in association with mitochondrial constriction sites. M, matrices of the mitochondria. (E) Dnm1 assembly in the presence of liposomes. Bars, 100 nm.

like structure around the circumference of mitochondria drives the constriction of outer and inner mitochondrial membranes (Tieu and Nunnari, 2000; Tieu et al., 2002). One prediction from this model is that the diameter of Dnm1 spirals would match the diameter of constricted mitochondria. To test this prediction, we characterized the structures that are formed by Dnm1 in the absence and presence of the nonhydrolyzable GTP analogue β,γ-methyleneguanosine 5′-triphosphate (GMP-PCP) by negative stain EM analysis (Fig. 5, A and B). In the absence of nucleotides or with added GDP, Dnm1 formed long, slightly curved filaments (Fig. 5 A). The addition of GMP-PCP to Dnm1, in contrast, promoted the assembly of ring and spiral-like structures (Fig. 5 B) that were similar to those observed for dynamin-1 (Fig. 5 B, inset). Strikingly, the mean diameter of Dnm1 spirals that formed in the presence of GMP-PCP (109 ± 16 nm; $n = 95$) was greater than dynamin-1 spirals (50 ± 12 nm) that formed under similar conditions (Fig. 5 B; Hinshaw and Schmid, 1995; Zhang and Hinshaw, 2001; Chen et al., 2004). The addition of GTP to GMP-PCP–Dnm1 spirals caused the disassembly of highly ordered rings into curved filaments that were similar to those seen in the absence of nucleotides, raising the possibility that conformational changes associated with disassembly may be used to facilitate fission (Fig. 5 C).

In vivo, immuno-EM analysis has shown that Dnm1 accumulates at sites of mitochondrial inner and outer membrane constriction, which are likely to be fission intermediates (Bleazard et al., 1999). To accurately determine the mean diameter of mitochondrial constriction sites in vivo, we analyzed thin sections of conventionally fixed yeast cells by EM. Late stage mitochondrial constriction sites were identified as regions where outer and inner mitochondrial membranes were coordinately constricted to the smallest observable diameter in the plane of the section (Fig. 5 D). The mean diameter of mitochondrial constriction sites in vivo was 109 ± 24 nm ($n = 100$), which is within the experimental error of the mean diameter of Dnm1 spirals. Significantly, the majority of constriction sites were associated with electron-dense structures, which, in some cases, clearly resembled in vitro Dnm1 spirals (Fig. 5 D, arrowheads).

To test more directly whether Dnm1 assembly can drive membrane constriction, we determined whether Dnm1 constricts artificial liposomes. The addition of Dnm1 to liposomes with diameters approximating those of unconstricted mitochondria (1.04 ± 0.55 μm; $n = 40$) in the presence of GMP-PCP caused them to constrict and form tubules with diameters of 111 ± 7 nm ($n = 40$), which also are within the range of diameters that were observed for in vivo mitochondrial constriction sites (Fig. 5 E). Thus, our data support a model in which the nucleation-dependent self-assembly of Dnm1 into spirals drives the constriction of mitochondria during division and further suggest that assembled DRPs have been structurally tailored to fit their target biological membranes.

It has been postulated that the master regulator of mitochondrial division is Dnm1 (Tieu and Nunnari, 2000; Shaw and Nunnari, 2002; Tieu et al., 2002). The observations presented in this study are consistent with this model and also with the idea that the self-assembly of Dnm1 spirals mediates constriction of mitochondrial membranes during division. Alternatively, but not exclusively, mitochondrial membrane constriction in vivo may require additional effectors such as Fis1 and Mdv1 and/or specific lipid modifications (Legesse-Miller et al., 2003). However, our findings emphasize the mechanistic importance of Dnm1 self-assembly in mitochondrial division and, thus, suggest a model in which the Fis1–Mdv1 complex triggers division by promoting the self-assembly of Dnm1 spirals on the mitochondrial outer membrane.

Materials and methods

Dnm1 protein expression and purification

Dnm1 was amplified from W303 genomic DNA by using primers 5′-CATGCCATGGCTATGGCTAGTTTAGAAGATCTTAT-3′ and 5′-GGGGTACCCTCGAGTTACAGAATATTACTAATAAGGGTTGCAGCC-3′. The GTPase domain expression vector was constructed by cloning a 1,164-bp fragment corresponding to aa 1–388 of Dnm1. The forward primer that was used to clone the GTPase domain of Dnm1 was the same as for full-length Dnm1; the reverse primer was 5′-ACGGCTCGAGTTACTTGGTTTTAATATCCGGAAGC-3′. After digestion with NcoI and XhoI (New England Biolabs, Inc.), PCR fragments were subsequently ligated into plasmid pFBNhis10HA (a gift from K. Kaplan, University of California, Davis, Davis, CA). Middle domain mutation G385D was introduced into Dnm1 by using standard

PCR mutagenesis with Pfu-Turbo (Boehringer). The composition of all plasmids was verified by DNA sequencing (University of California Davis Sequencing Facility, Davis, CA).

The resultant plasmids were transformed into DH10Bac cells, from which a bacmid was extracted. By using Transfection Buffer Set A and B (BD Biosciences), purified bacmid was transfected into sf9 insect cells. Primary virus was collected after 5 d. Primary viral stocks were amplified in sf9 cells, and high titer virus was used for protein expression in Hi5 insect cells. Infected Hi5 cells were collected after ~48 h of infection and were stored at −80°C. Infected cells were thawed at RT and resuspended in wash buffer (25 mM Hepes, 25 mM Pipes, pH 7.0, 500 mM NaCl, and 80 mM imidazole, pH 7.4) containing protease inhibitor cocktail 1 (Calbiochem). Resuspended thawed cells were lysed by passage through a 21-g/1-inch needle and two passages through a 27-g/0.5-inch needle. The lysate was centrifuged at 60,000 *g* for 30 min, and Dnm1 was purified from the supernatant using a HiTrap metal chelating column attached to an AKTA prime system (GE Healthcare). Dnm1 was eluted from the column by using a linear gradient of 25 mM Hepes, 25 mM Pipes, pH 7.0, 500 mM NaCl, and 500 mM imidazole, pH 7.4. DMSO was added to purified Dnm1 to a final concentration of 20% (vol/vol), rendering the freezing buffer 20 mM Hepes, 20 mM Pipes, 400 mM imidazole, and 20% DMSO. Purified protein was frozen in liquid nitrogen and stored at −80°C.

GTPase assay

We used a coupled assay in which GTP was continuously regenerated from GDP by the enzyme pyruvate kinase, using phosphoenolpyruvate (PEP) as a substrate (Renosto et al., 1984). In this reaction, pyruvate kinase produces pyruvate, which, in turn, is reduced to lactate by the enzyme lactate dehydrogenase and simultaneously depletes pyruvate's cosubstrate NADH. Depletion of NADH was measured by monitoring absorbance at 340 nm. The change in absorbance over time was used to calculate steady-state GTPase activity under the initial constant substrate concentration.

For determination of kinetic parameters, GTPase assays were performed in 25 mM Hepes, 25 mM Pipes, pH 7.0, 30 mM imidazole, pH 7.4, 7.5 mM KCl, 5 mM $MgCl_2$, 1 mM PEP, 20 U/ml pyruvate kinase/lactate dehydrogenase, and 600 μM NADH. 30–750 mM NaCl and 10–1,000 μM GTP concentrations were varied as required. GTPase assay reactions were started by the addition of ~10 μg of purified protein in freezing buffer to the GTPase assay reaction buffer.

For examination of the lag with respect to protein concentration, purified Dnm1 and Dnm1G385D were first exchanged into 25 mM Hepes, 25 mM Pipes, pH 7.0, and 500 mM NaCl by using a HiTrap desalting column (GE Healthcare) to remove excess imidazole, which has an inhibitory effect on GTPase activity. GTPase assays were performed in 25 mM Hepes, 25 mM Pipes, pH 7.0, 7.5 mM KCl, 187.5 mM NaCl, 5 mM $MgCl_2$, 1 mM PEP, 20 U/ml pyruvate kinase/lactate dehydrogenase, 500 μM GTP, and 800 μM NADH.

All GTPase assay reactions were performed in 200-μl volumes, of which 150 μl was placed into wells of a 96-well plate. Depletion of NADH over time was measured during 40 min by using a 96-well plate reader (SpectraMAX 250; Molecular Devices). Spectrophotometric data were transferred to Microsoft Excel, and the measured depletion of NADH over time was converted to a protein activity. $K_{0.5}$, K_m, k_{cat}, and Hill coefficient were calculated numerically by using the Genfit function of Mathcad.

Velocity sedimentation of Dnm1

0.76 mg/ml of purified Dnm1 was diluted 1:10 to low and high ionic strength, incubated on ice for 15 min, and centrifuged for 15 min at 50,000 *g* using a rotor (model TLA 100.4; Beckman Coulter) in an ultracentrifuge (Optima TLX; Beckman Coulter). Final buffer conditions were 25 mM Hepes, 25 mM Pipes, pH 7.0, and 40 mM NaCl (low ionic strength) or 600 mM NaCl (high ionic strength). After centrifugation, supernatants were removed, and pellets were resuspended in a volume of sample buffer equal to that of the supernatant. Equal volumes of supernatant and resuspended pellet were diluted 1:1 with sample buffer and resolved on a 12.5% SDS-PAGE gel, and Dnm1 was visualized by silver staining.

Hydrodynamic analyses

10 ml of 5–20% and 10–30% sucrose gradients were used for hydrodynamic measurements and contained 25 mM Hepes, 25 mM Pipes, pH 7.0, 500 mM NaCl, 10% (vol/vol) DMSO, and 1 mM DTT. 300-μl volumes of protein sample containing 5% sucrose, 25 mM Hepes, 25 mM Pipes, pH 7.0, 500 mM NaCl, 10% DMSO, and 1 mM DTT were loaded on top of the sucrose gradient. Sucrose gradients were centrifuged using a SW41 Ti rotor (Beckman Coulter) in an ultracentrifuge (Optima XL-100K; Beckman Coulter) for 14.5 h at 40,000 rpm and 4°C using acceleration and deceleration settings of 5. 10 1-ml fractions were collected from the top for analysis.

Molecular mass markers with known sedimentation coefficients (17–0445-01; GE Healthcare) that were simultaneously run over separate sucrose gradients were used to construct standard curves of fraction number versus sedimentation coefficient and to estimate the Svedberg coefficients of Dnm1, Dnm1G385D, and $Dnm1^{1–388}$. To determine Stokes' radii, purified protein was chromatographed on a Superose 6 column using an AKTA prime system (GE Healthcare). Gel filtration standards (Bio-Rad Laboratories) with known Stokes' radii were also chromatographed. For each protein component of gel filtration standards, values of $K_d^{1/3}$ were plotted versus Stokes' radii in order to construct a Porath correlation standard curve. Molecular mass was calculated from combined sucrose gradient and gel filtration data by using the method developed by Siegel and Monty (1966).

EM

Dnm1 structural analysis in vitro. To prepare negative stain specimens, a carbon-coated grid was placed on a 10-μl sample drop of protein for 2 min, blotted with filter paper, stained with 2% uranyl acetate for 2 min, blotted again, and air dried. For GMP-PCP experiments, Dnm1 was dialyzed into 1 mM GMP-PCP overnight at 4°C and examined by negative stain microscopy. To prepare cryo-EM images of Dnm1–lipid tubes, a 9:1 ratio of DOPE and phosphatidylethanolamine (Avanti Polar Lipid, Inc.) were dried under nitrogen gas and kept in a vacuum overnight before solubilization in buffer to a final total lipid concentration of 2 mg/ml. Lipid was added with Dnm1 and incubated at RT for 2 h. GMP-PCP was added to a final concentration of 1 mM and allowed to incubate for 15 min. The sample was added to a Quantifoil grid and rapidly frozen in liquid ethane using the Vitrobot system (FEI Co.). All images were obtained from a transmission electron microscope (Philips CM120; FEI Co.) operating at 100 kV and were taken at 35,000× for negative stained samples and 110,000× for cryo-EM with a focus range of 0.8–1.5 mm underfocus. Images were recorded digitally on CCD cameras (MultiScan 791 and 794; Gatan) with the Digital Micrograph software package (Gatan; Danino et al., 2004).

Analysis of mitochondrial constriction sites in vivo. Conventional EM was performed essentially as previously described (Rieder et al., 1996). The cells were fixed in 3% glutaraldehyde contained in 0.1 M nacacodylate, pH 7.4, 5 mM $CaCl_2$, 5 mM $MgCl_2$, and 2.5% sucrose for 1 h at 25°C with gentle agitation. Then, cells were spheroplasted, embedded in 2% (wt/vol) ultra low temperature agarose, cooled, and subsequently cut into small pieces (~1 mm^3). The cells were postfixed in 1% OsO_4/1% potassium ferrocyanide contained in 0.1 M cacodylate/5 mM $CaCl_2$, pH 7.4, for 30 min at RT. The blocks were washed thoroughly four times with double distilled H_2O for 10 min, transferred to 1% thiocarbohydrazide at RT for 3 min, washed in double distilled H_2O (four times for 1 min), and transferred to 1% OsO_4/1% potassium ferrocyanide in cacodylate buffer, pH 7.4, for an additional 3 min at RT. The cells were then washed four times with double distilled H_2O for 15 min, en bloc stained in Kellenberger's uranyl acetate for 2 h to overnight, dehydrated through a graded series of ethanol, and subsequently embedded in Spurr resin. Sections were cut on an ultramicrotome (Ultracut T; Reichert), poststained with uranyl acetate and lead citrate, and observed on a transmission electron microscope (TEM 420; Philips) at 80 kV. Images were recorded with a digital camera (Megaview III; Soft Imaging System), and figures were assembled in Adobe Photoshop 7.0.

For quantitative analysis of mitochondrial constriction sites, 100 images were collected of conventionally sectioned mitochondria with well-defined constrictions, which were defined as constrictions having both well-defined outer and inner membranes. The constriction diameter was measured by using analySIS 3.2 software (Soft Imaging System), and the mean diameter was calculated by using Microsoft Excel.

Purification of dynamin-1

Plasmid pFB-HT-Dyn1 for the expression of dynamin in insect cells was obtained from M. Lemmon (University of Pennsylvania, Philadelphia, PA). Dynamin-1 was purified as described for Dnm1.

Online supplemental material

Supplemental figures provide additional in vitro characterizations of Dnm1, Dnm1G385D, and dynamin. Fig. S1 shows the dependence of GTPase activity on the concentration of Dnm1 and Dnm1G385D. Fig. S2 shows the time dependence of dynamin-1 GTPase activity under self-assembly conditions, and Fig. S3 shows that Dnm1 GTPase activity is inhib-

ited by Dnm1G385D. Online supplemental material is available at http://www.jcb.org/cgi/content/full/jcb.200506078/DC1.

We are grateful to Dr. Irwin Segel for his critical advice.

This work was support by NIH grants 1R01EY015924 and 5R01GM062942 to J. Nunnari. E. Ingerman is supported by NIH training grant 5T32GM007377.

Submitted: 14 June 2005
Accepted: 9 August 2005

References

Bleazard, W., J.M. McCaffery, E.J. King, S. Bale, A. Mozdy, Q. Tieu, J. Nunnari, and J.M. Shaw. 1999. The dynamin-related GTPases, Dnm1, regulates mitochondrial fission in yeast. *Nat. Cell Biol.* 1:298–304.

Cerveny, K.L., and R.E. Jensen. 2003. The WD-repeats of Net2p interact with Dnm1p and Fis1p to regulate division of mitochondria. *Mol. Biol. Cell.* 14:4126–4139.

Cerveny, K.L., J.M. McCaffery, and R.E. Jensen. 2001. Division of mitochondria requires a novel DNM1-interacting protein, Net2p. *Mol. Biol. Cell.* 12:309–321.

Chen, Y.J., P. Zhang, E.H. Egelman, and J.E. Hinshaw. 2004. The stalk region of dynamin drives the constriction of dynamin tubes. *Nat. Struct. Mol. Biol.* 11:574–575.

Danino, D., K.H. Moon, and J.E. Hinshaw. 2004. Rapid constriction of lipid bilayers by the mechanochemical enzyme dynamin. *J. Struct. Biol.* 147:259–267.

Fekkes, P., K.A. Shepard, and M.P. Yaffe. 2000. Gag3p, an outer membrane protein required for fission of mitochondrial tubules. *J. Cell Biol.* 151: 333–340.

Fukushima, N.H., E. Brisch, B.R. Keegan, W. Bleazard, and J.M. Shaw. 2001. The AH/GED sequence of the dnm1p GTPase regulates self-assembly and controls a rate-limiting step in mitochondrial fission. *Mol. Biol. Cell.* 12:2756–2766.

Griffin, E.E., J. Graumann, and D.C. Chan. 2005. The WD40 protein Caf4p is a component of the mitochondrial fission machinery and recruits Dnm1p to mitochondria. *J. Cell Biol.* 170:237–248.

Hinshaw, J.E. 2000. Dynamin and its role in membrane fission. *Annu. Rev. Cell Dev. Biol.* 16:483–519.

Hinshaw, J.E., and S.L. Schmid. 1995. Dynamin self-assembles into rings suggesting a mechanism for coated vesicle budding. *Nature.* 374:190–192.

Jensen, R.E., A.E. Hobbs, K.L. Cerveny, and H. Sesaki. 2000. Yeast mitochondrial dynamics: fusion, division, segregation, and shape. *Microsc. Res. Tech.* 51:573–583.

Kim, Y.W., D.S. Park, S.C. Park, S.H. Kim, G.W. Cheong, and I. Hwang. 2001. *Arabidopsis* dynamin-like 2 that binds specifically to phosphatidylinositol 4-phosphate assembles into a high-molecular weight complex in vivo and in vitro. *Plant Physiol.* 127:1243–1255.

Kochs, G., M. Haener, U. Aebi, and O. Haller. 2002. Self-assembly of human MxA GTPase into highly ordered dynamin-like oligomers. *J. Biol. Chem.* 277:14172–14176.

Legesse-Miller, A., R.H. Massol, and T. Kirchhausen. 2003. Constriction and Dnm1p recruitment are distinct processes in mitochondrial fission. *Mol. Biol. Cell.* 14:1953–1963.

Marks, B., M.H.B. Stowell, Y. Vallis, I.G. Mills, A. Gibson, C.R. Hopkins, and H.T. McMahon. 2001. GTPase activity of dynamin and resulting conformational change are essential for endocytosis. *Nature.* 410:231–234.

Mozdy, A.D., J.M. McCaffery, and J.M. Shaw. 2000. Dnm1p GTPase-mediated mitochondrial fission is a multi-step process requiring the novel integral membrane component Fis1p. *J. Cell Biol.* 151:367–380.

Muhlberg, A.B., D.E. Warnock, and S.L. Schmid. 1997. Domain structure and intramolecular regulation of dynamin GTPase. *EMBO J.* 16:6676–6683.

Narayanan, R., M. Leonard, B.D. Song, S.L. Schmid, and M. Ramaswami. 2005. An internal GAP domain negatively regulates presynaptic dynamin in vivo: a two-step model for dynamin function. *J. Cell Biol.* 169:117–126.

Newmyer, S.L., A. Christensen, and S. Sever. 2003. Auxilin-dynamin interactions link the uncoating ATPase chaperone machinery with vesicle formation. *Dev. Cell.* 4:929–940.

Osteryoung, K.W., and J. Nunnari. 2003. The division of endosymbiotic organelles. *Science.* 302:1698–1704.

Praefcke, G.J., and H.T. McMahon. 2004. The dynamin superfamily: universal membrane tubulation and fission molecules? *Nat. Rev. Mol. Cell Biol.* 5:133–147.

Renosto, F., P.A. Seubert, and I.H. Segel. 1984. Adenosine 5′-phosphosulfate kinase from penicillium chrysogenum. Purification and kinetic characterization. *J. Biol. Chem.* 259:2113–2123.

Rieder, S.E., L.M. Banta, K. Kohrer, J.M. McCaffery, and S.D. Emr. 1996. Multilamellar endosome-like compartment accumulates in the yeast vps28 vacuolar protein sorting mutant. *Mol. Biol. Cell.* 7:985–999.

Sever, S., A.B. Muhlberg, and S.L. Schmid. 1999. Impairment of dynamin's GAP domain stimulates receptor-mediated endocytosis. *Nature.* 398:481–486.

Sever, S., H. Damke, and S.L. Schmid. 2000. Dynamin: GTP controls the formation of constricted coated pits, the rate limiting step in clathrin-mediated endocytosis. *J. Cell Biol.* 150:1137–1147.

Shaw, J.M., and J. Nunnari. 2002. Mitochondrial dynamics and division in budding yeast. *Trends Cell Biol.* 12:178–184.

Siegel, L.M., and K.J. Monty. 1966. Determination of molecular weights and frictional ratios of proteins in impure systems by use of gel filtration and density gradient centrifugation. Application to crude preparations of sulfite and hydroxylamine reductases. *Biochim. Biophys. Acta.* 112:346–362.

Smirnova, E., D.-L. Shurland, E.D. Newman-Smith, B. Pishvaee, and A.M. van der Bliek. 1999. A model for dynamin self-assembly based on binding between three different protein domains. *J. Biol. Chem.* 274:14942–14947.

Song, B.D., and S.L. Schmid. 2003. A molecular motor or a regulator? Dynamin's in a class of its own. *Biochemistry.* 42:1369–1376.

Song, B.D., D. Yarar, and S.L. Schmid. 2004. An assembly-incompetent mutant establishes a requirement for dynamin self-assembly in clathrin-mediated endocytosis in vivo. *Mol. Biol. Cell.* 15:2243–2252.

Suzuki, M., A. Neutzner, N. Tjandra, and R.J. Youle. 2005. Novel structure of the N terminus in yeast Fis1 correlates with a specialized function in mitochondrial fission. *J. Biol. Chem.* 280:21444–21452.

Takei, K., V. Haucke, V. Slepnev, K. Farsad, M. Salazar, H. Chen, and P. De Camilli. 1998. Generation of coated intermediates of clathrin-mediated endocytosis on protein-free liposomes. *Cell.* 94:131–141.

Tieu, Q., and J. Nunnari. 2000. Mdv1p is a WD repeat protein that interacts with the dynamin-related GTPase, Dnm1p, to trigger mitochondrial division. *J. Cell Biol.* 151:353–365.

Tieu, Q., V. Okreglak, K. Naylor, and J. Nunnari. 2002. The WD repeat protein, Mdv1p, functions as a molecular adaptor by interacting with Dnm1p and Fis1p during mitochondrial fission. *J. Cell Biol.* 158:445–452.

van der Bliek, A.M. 1999. Functional diversity in the dynamin family. *Trends Cell Biol.* 9:96–102.

Warnock, D.E., J.E. Hinshaw, and S.L. Schmid. 1996. Dynamin self-assembly stimulates its GTPase activity. *J. Biol. Chem.* 271:22310–22314.

Yoon, Y., K.R. Pitts, and M.A. McNiven. 2001. Mammalian dynamin-like protein DLP1 tubulates membranes. *Mol. Biol. Cell.* 12:2894–2905.

Zhang, P., and J.E. Hinshaw. 2001. Three-dimensional reconstruction of dynamin in the constricted state. *Nat. Cell Biol.* 3:922–926.

Zhang, Z., Z. Hong, and D.P. Verma. 2000. Phragmoplastin polymerizes into spiral coiled structures via intermolecular interaction of two self-assembly domains. *J. Biol. Chem.* 275:8779–8784.

Zhu, P.P., A. Patterson, J. Stadler, D.P. Seeburg, M. Sheng, and C. Blackstone. 2004. Intra- and intermolecular domain interactions of the C-terminal GTPase effector domain of the multimeric dynamin-like GTPase Drp1. *J. Biol. Chem.* 279:35967–35974.